Journal of Nuclear Materials 84 (1979) 109–117

THE CHEMICAL STATE OF LWR HIGH-POWER RODS UNDER IRRADIATION *

H. KLEYKAMP

Kernforschungszentrum Karlsruhe, Institut für Material- und Festkörperforschung, Postfach 3640, 7500 Karlsruhe, Fed. Rep. Germany

Received 28 March 1979

A section of a high-power fuel rod irradiated in the KWO reactor to 4.3% burnup at a mean linear rating of 43 kW/m has been investigated by electronprobe microanalysis. The concentrations of the converted plutonium and the most important fission products dissolved and precipitated in the fuel are given as a function of the fuel radius. The radial xenon release is evaluated. The oxygen concentration profile in the zircaloy cladding is determined. The reaction layers at the inner cladding surface are apparently α-Zr(O) and a Cs–Zr–O phase. The radial dependence of the EOL fuel stoichiometry is calculated using the composition of metallic fission product precipitates, the oxidation state of steel impurities and the oxygen content of the α-Zr(O) phase, which results in a constant O/M = 2.00 over the whole fuel radius.

1. Introduction

While studies of irradiated LMFBR mixed-oxide fuel pins extending over many years have already produced a clear picture of their chemical state [16], information about the chemical behaviour of LWR fuel rods is still very incomplete. Detailed work on the reaction behaviour of the fuel relative to the fission products and the cladding has only recently started on irradiated material. So far, most attention has been directed to the problems of the shift in stoichiometry of irradiated fuel and the radial stoichiometry profile [1] and to the reaction behaviour of the zircaloy cladding under the influence of volatile fission products [2,3].

In principle, the problems of the reaction behaviour and the thermodynamics of irradiated LWR fuels are similar to those associated with LMFBR mixed-oxide fuels. However, there are slight differences because LWR fuels have to be considered always in connection with the zircaloy cladding due to the oxygen gettering effect of this alloy whereas oxygen originating from LMFBR mixed-oxide fuels participates in reactions with the steel cladding at higher operation temperatures resulting in extensive oxide phases or corrosive zones visible under the optical microscope.

The investigations on a LWR fuel-pin section selected for the present must be viewed against the background of the experience accumulated in the analysis of numerous irradiated LMFBR mixed oxide fuel rods. In order to approximate thermodynamic equilibrium in the fuel and make it feasible to detect as quantitatively as possible the influence of fission products, a section of a high-power fuel pin (HLB) from a special subassembly of the Obrigheim Nuclear Power Station (KWO) was chosen which, at a rod power greater than 40 kW/m and a high center temperature (1800°C), had reached a burnup in excess of 4%.

The studies were carried out with the shielded electronprobe microanalyzers MS46 made by Cameca and JRXA-50 made by Jeol.

2. Frabrication and irradiation data of the specimen

The section selected was prepared metallographically at KWU Erlangen; it was photographed and ground, in order to reduce the dose rate to workable levels. During this operation, a narrow section of fuel was lost. At the time of investigation the β–γ dose

* Paper presented at the Specialist's Meeting on Internal Fuel Rod Chemistry, Erlangen, 23–25 January, 1979. The complete documentation is given in the report KfK 2696 (1979).

Table 1
Fabrication and irradiation data of the 41.247.45MK03-1 specimen

Fuel data	
Fuel	UO_2 with 6% of U-235/total U
Stoichiometry	O/U = 2.003
Pellet diameter	9.08 mm
Fuel density	92%
Fuel rod data	
Radial gap	110 μm
Fuel rod diameter	10.75 mm
Thickness of cladding tube wall	0.70 mm
Cladding material	Zircaloy-4
Internal pre-pressure	28 bar of He
Irradiation data	
Mean temperature of outside cladding tube	342°C
Mean local rod power	43 kW/m
Local burnup	41 MWd/kgU = 4.3%
Irradiation time	October 1972–August 1974 (4th and 5th cycle), 607 days of full power
Flux, 4th cycle:	1.4×10^{14} n/cm^2 · s (1.2 eV–10 MeV)
	0.4×10^{14} n/cm^2 · s (0.001 eV–1.2 eV)
5th cycle:	2.6×10^{14} n/cm^2 · s (1.2 eV–10 MeV)
	0.8×10^{14} n/cm^2 · s (0.001 eV–1.2 eV)

rate of the specimen as determined in Karlsruhe was about 80 mrem/h at a distance of 30 cm. The fabrication and irradiation data were taken from ref. [4] and are compiled in table 1.

Diametral point analyses of some fission products were obtained in two directions normal to each other so as to allow any radial asymmetry of the positions of the pellets in the rod or of the flux to be detected.

3. Plutonium distribution

The plutonium distribution was measured across the diameter of the fuel rod as a concentration profile. The curve (fig. 1) with a maximum value of 1.3% PuO_2 on the fuel surface reflects the flux depression which, in a LWR, is much flatter than in a thermal MTR (such as FR 2). The mean value is 0.8% PuO_2, which is the difference between the converted and the plutonium then partly burned in $^{238}U_{0.94}{}^{235}U_{0.06}O_2$ fuel after 4.3% burnup. The UO_2 concentration (fig. 1) is much lower in the regions close to the surface of the fuel than would correspond to the radial fission density distribution. The reason for this is due to increased concentration of some fission products in this region (see section 4) which make up the difference between UO_2 plus PuO_2 and 100%. From the zirconium profile of the cladding material (fig. 1), it is deduced that the position of the fuel pellet was concentric in the fuel rod.

4. Distribution and precipitation behaviour of condensed fission products

The distributions of cesium, molybdenum, zirconium and xenon (see section 5) were measured partly in two profile directions, by means of point analysis (fig. 2) as a function of the fuel diameter.

On the basis of thermodynamic estimates of the oxygen potential of the fuel, the thermodynamics in the Cs–O system [5] and the phase diagram of the Cs–U–O system [6], cesium can be assumed to be present inside the fuel during irradiation as a Cs–O melt and as Cs_2UO_4. A semi-quantitative analysis of the ternary compound succeeded only on one sufficiently large precipitate. In most cases it was found that cesium is submicroscopically distributed in the pores and cracks of the fuel.

At low oxygen potentials of the fuel (see section 10) most of the molybdenum is contained in the Mo–Tc–Ru–Rh–Pd alloys. The shape of the curve in fig. 2 represents the concentration, averaged over the unit area, of submicroscopically precipitated molybdenum containing phases invisible under the optical microscope. The major fraction is found in the visible metallic inclusions. They are biphase; molybdenum and ruthenium behave in a complementary way (phases D and E in fig. 3), while the concentrations of technetium, rhodium and palladium are almost constant in the two phases of an inclusion. From the molybdenum concentration level in the metallic precipitates, information can be derived on the final stoichiometry of the fuel (see section 10 and refs. [7,16]).

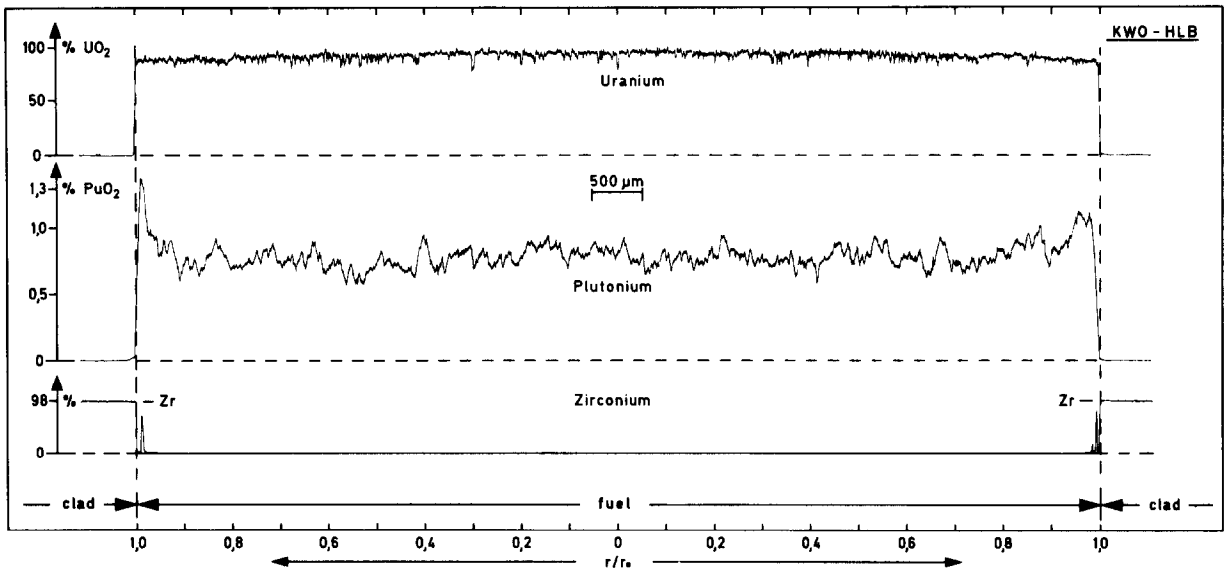

Fig. 1. Diametral concentration profiles of uranium, plutonium and zirconium across the fuel pin.

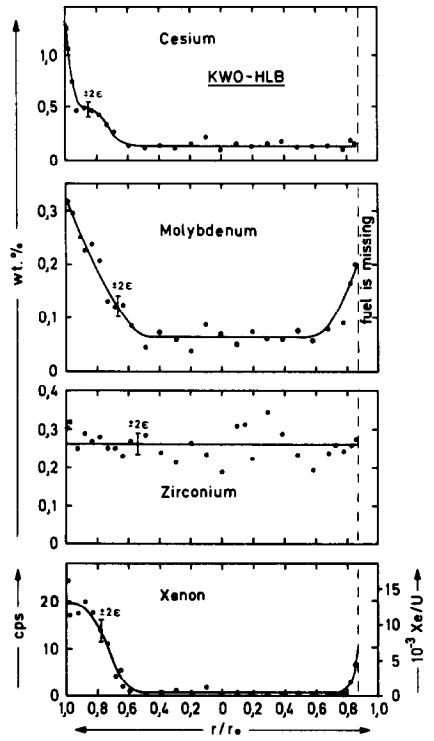

Fig. 2. Diametral concentration profiles by point analysis of cesium and molybdenum submicroscopically precipitated in the fuel, and of zirconium dissolved and xenon bonded in the fuel (in 10^{-3} Xe atoms per U atom); $\pm 2\sigma$ = 95% confidence limit.

Zirconium is contained in the fuel mainly in dissolved form; however, the analysis does not take into account the fraction precipitated as zirconates.

The radially symmetric distribution of fission products does not give any indication of eccentric pellet positions or unbalanced loads. The comparison between

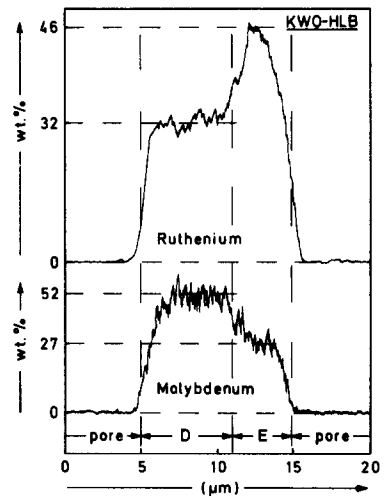

Fig. 3. Concentration profiles of the main constituents molybdenum and ruthenium of a two-phase metallic fission product precipitate (phases D and E).

Table 2
Comparison of the calculated fission product yields and the concentrations determined by electronprobe microanalysis

Fission product	Calculated [8] (%)	Measured (%)
Cs	0.32	0.30
Mo	0.41	≈0.2 b)
Zr	0.45	0.27 c)
Xe	0.35 a)	0.35

a) Retained fraction only (50% of the xenon created [4])
b) Does not include the molybdenum fraction in the visible metallic precipitates
c) Does not include the zirconium fraction in the zirconate precipitates.

calculated fission product concentrations in the fuel [8] and those determined by electronprobe microanalysis averaged over the radius is seen in table 2.

5. Distribution of bonded fission gas

It has already been shown in [9,10] that the radial distribution of retained xenon (the sum total of lattice and microbubble xenon) was determined by point analysis in relative units, i.e., by the count rate (cps) which can be calibrated at the level of the section by integral gas chromatographic measurements and by burnup analysis of the total fission gas.

The fission gas release is indicated to be 50% for the HLB rod [4]. Since the axial rod power and burnup curves are constant and show a steep decline only at the fuel ends, it can be assumed that the fission gas release level is also valid for the cross-section studied from the middle of the rod. From the total amount of fission gas, from the Xe/Kr ratio, the relative Xe release and the original amount of fuel, it is possible to calculate the fractional retained xenon averaged over the fuel radius: it is 6.1×10^{-3} Xe atoms per initial U atom. This value corresponds to the area under the curve obtained when plotting cps versus $(r/r_0)^2$.

The fractional xenon distribution has been plotted as a function of the fuel diameter in fig. 2. The xenon concentration was not measured at the right hand edge of the pellet because of the material missing. The fractional xenon release as a function of the fuel radius was converted from the left hand part of the curve in fig. 2 with the normalization condition of 12.2×10^{-3} Xe/U $\hat{=}$ 0% release, and is shown in fig. 4.

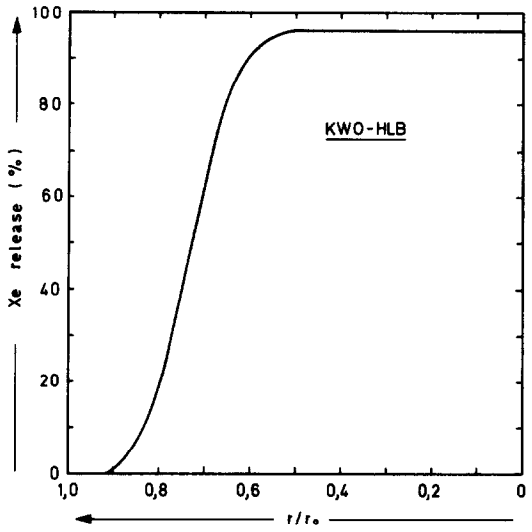

Fig. 4. Relative xenon release vs. relative fuel radius.

In the fuel region greater than $0.9r_0$ apparently all xenon is present in the bonded form. Towards the fuel center the amount of xenon released increases greatly, reaching values up to 96%. A small fraction of 4% remains bonded in the center of the fuel at temperatures of 1800°C (see section 9).

6. Impurities in the fuel

Some steel precipitates were observed in the fuel which were partly oxidized during irradiation. This is high Cr–Ni steel out of which chromium was partly oxidized as Cr_2O_3. The composition of one inoxidized residue is 77% Fe, 11% Ni, 6% Cr with minor fractions of Mn and Mo. Assuming thermal equilibrium with the surrounding fuel, the local oxygen potential can be calculated from the degree of oxidation of these precipitates, which makes it possible to indicate the local stoichiometry of the fuel at the end of irradiation (see section 10).

7. Reactions of fission products with the zircaloy cladding

The reactions of volatile fission products with the cladding material are subject of numerous studies in

unpublished reports and in the unclassified literature [2,3]. Even the first tentative analyses (figs. 5 and 6) show by relative concentration profiles and element distribution images, that the elements U, Zr and Cs exist side by side in the gap region between the fuel and the cladding, but that there is no complete coincidence. Especially from the concentration profiles of cesium and zirconium in fig. 5, information was derived about a two-phase character of the precipitates but, because of lacking oxygen analysis, the exact composition of the phases could not be identified. These questions are clearly answered by fig. 6. The precipitates between the fuel and the cladding are mostly two-phase in nature, consisting of an oxidic cesium–zirconium phase (perhaps a Cs–Zr oxide bronze, phase A) and of α-Zr(O) or ZrO_2 (phase B), but the quantitative determination of the latter phase remained unsatisfactory because it was located below the surface of the section. The composition is shown in table 3.

In the post-irradiation examinations of irradiated LWR fuel rods the formation of Cs_2ZrO_3 of Cs_2ZrO_4 phases was supposed in various reports. These compounds, however, have not been described in the literature. Hoppe and Seeger [11] indicate the structural properties of Rb_2ZrO_3, but this easily decomposes in air. So, it cannot be excluded that isotypic Cs_2ZrO_3 is formed in irradiated LWR fuel rods, which, however, cannot be detected because of its instability. On the other hand, the measured composition of the Cs–Zr–O phase (table 3) in no way agrees with that of the presumed compound, Cs_2ZrO_3 (66% Cs, 23% Zr, 12% O). Hence, it must be assumed, for the time being that cesium exists as any oxidic Cs–Zr–O phase (perhaps as a bronze). In addition, there is ZrO_2 or pure α-Zr(O) on the cladding side with higher oxygen concentrations from which, on the assumption of thermodynamic equilibrium with the adjacent fuel, the local oxygen potential and the stoichiometry at the fuel surface at the end of irradiation can be calculated (see section 10).

8. Oxygen in the zircaloy cladding

The concentration profile of the oxygen diffusing from the fuel into the cladding was determined by

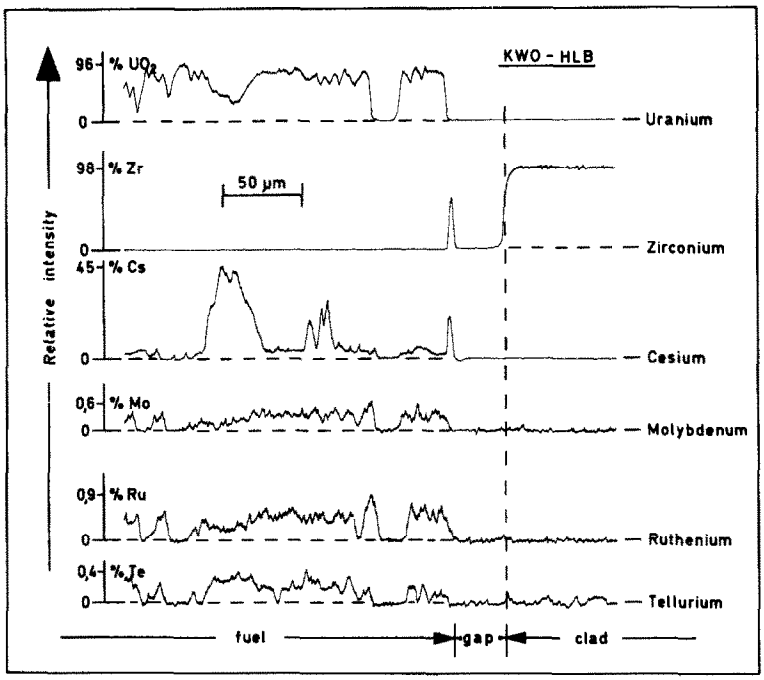

Fig. 5. Relative concentration profiles of uranium, zirconium and selected fission products between the fuel surface region and the cladding which are indicative of cesium uranate and ceramic cesium–zirconium phases.

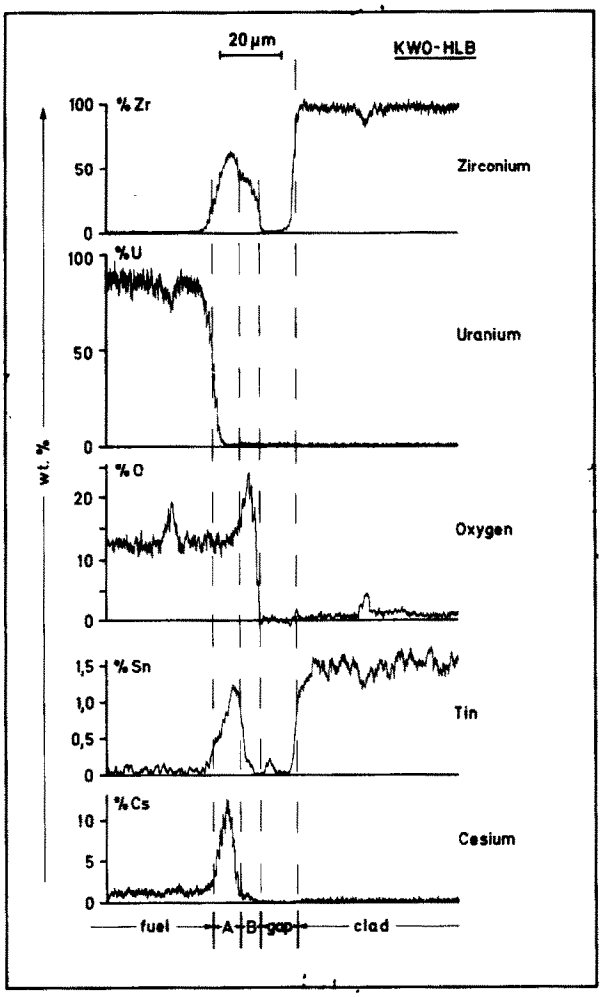

Fig. 6. Concentration profiles across ceramic cesium and zirconium bearing phases in the gap between the fuel and the cladding. Phase A: Cs–Zr–Sn–O layer; phase B: α–Zr(O) or ZrO_2.

point analyses in two positions (fig. 7). The quantitative analysis was performed with a zircaloy standard with 0.13% of oxygen. The oxygen concentration is 2.2% O at the inner cladding surface dropping to a

Table 3
Composition of the precipitations on the inside of the cladding; corrected, unnormalized concentrations in wt% (fig. 6)

Phase	Zr	O	Cs	Sn
A	70	14	13	1
B	45	23	0	0

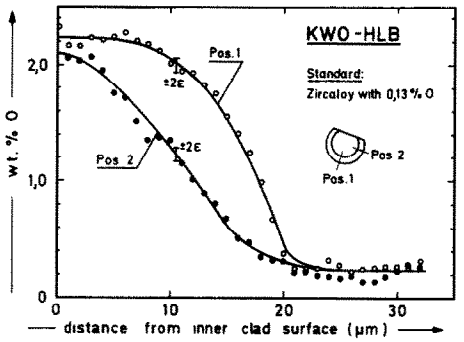

Fig. 7. Oxygen penetrated into zircaloy as a function of the distance from the inner cladding surface; $\pm 2\epsilon$ = 95% confidence limit.

constant level of 0.26% O in the interior. Some of the oxygen originates from the slightly hyperstoichiometric fuel at the onset of irradiation, some from the fraction that was not bound by the fission products during burnup. The measured profile should ideally be compared with the calculated one. However, the calculation is aggravated by the fact that the diffusion path is not an isotherm and the oxygen concentration at the inner cladding surface increases in a non-linear way with burnup.

The zircaloy cladding was oxidized in a crescent shape fashion from the outside. The maximum thickness of the ZrO_2 layer formed is 80 µm. The morphology of the ZrO_2 is flaky, because of its higher specific volume. The layer is permeated by small tangential

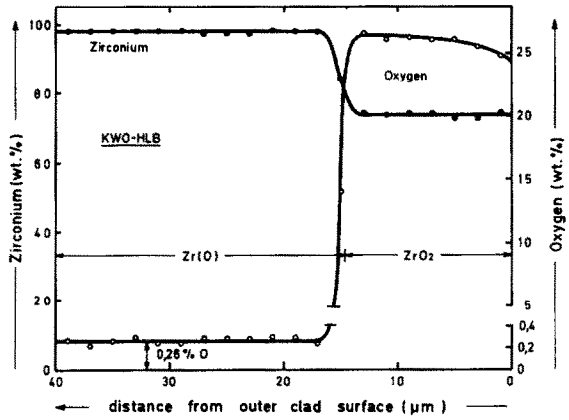

Fig. 8. Concentration profiles by point analysis of zirconium and oxygen as a function of the distance from the outer cladding surface.

cracks. At another position of the crescent with a thinner ZrO_2 layer about 15 μm thick, concentration of profiles of zirconium and oxygen were obtained by point analyses as a function of distance from the outer edge of the cladding (fig. 8). The mean oxygen concentration of 26% corresponds to the theoretical value in ZrO_2. It quickly drops to 0.26% O in the following α-Zr(O) region. This value resulted with the available zircaloy standard and must be backed by analyses of other specimens.

9. Thermal analysis

The radial fuel temperature profile of the section was calculated by the SATURN 3 computer program [12], taking into account the radial flux depression in LWR fuel rods [13]. Besides the data compiled in table 1, the following values were used: heat transfer coefficient through the gap: 1.2 W/cm²K; radial cold gap (EOL): 30 μm; thermal conductivity of the cladding: 0.17 W/cm · K. The fuel porosity was subdivided into two zones: $r < 0.6r_0$ with 89% theoretical density; $r \geqslant 0.6r_0$ with 96% theoretical density. It was assumed that the position of the pellet during reactor operation remained concentric. The radial temperature profiles are shown in fig. 9. Without flux depression, a central temperature of 1850°C is found. If a flux depression is taken into account [13], the result is

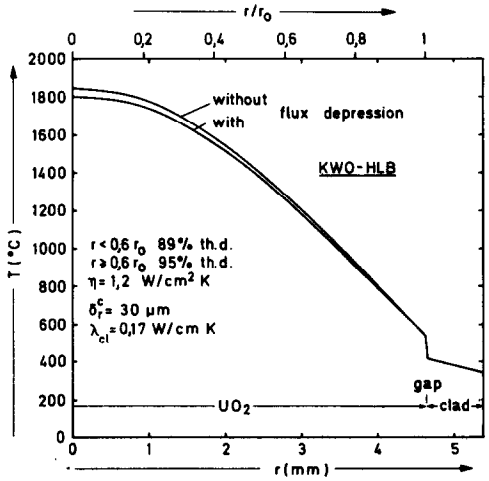

Fig. 9. Radial temperature distribution in the fuel neglecting and considering the neutron flux depression.

1790°C. Equiaxed grain growth can be seen in the microstructure of the central fuel region. According to the thermal analysis, columnar grains should be formed only above 1800°C.

10. Radial dependence of fuel stoichiometry at the end of irradiation

Various methods have been suggested to determine the radial dependence of the EOL fuel stoichiometry; the most successful technique to be applied to irradiated LMFBR mixed oxide is based on calculating the oxygen potential from the molybdenum concentration in the alloy phases and the molybdenum dioxide concentration in the oxide precipitates [7]. In LWR fuel rods with low fuel temperatures, the MoO_2 bearing ceramic precipitates are too small for quantitative analysis. However, the concentration of molybdenum in the metallic precipitates allows a semi-quantitative statement to be made about the local oxygen potential [16].

The high molybdenum concentration and the two-phase character of the precipitates in the sample investigated are already indicative of a very low oxygen potential in the fuel. At the point $r = 0.15r_0$ of the relative fuel radius (r_0 = pellet radius) with a fuel temperature of 2000 K resulting from thermal analysis, 52% Mo was measured in the molybdenum rich phase, 27% Mo in the phase with the lower molybdenum content (fig. 3).

These concentrations are similar to those in the precipitates up to $r = 0.5r_0$. According to ref. [7], the molybdenum contents correspond to an oxygen potential of −90 to −100 kcal/mol O_2. At $r = 0.90r_0$ (T = 1000 K), a partly oxidized steel impurity was observed of which it is assumed that oxidation occurred during irradiation (see section 6). Chromium as Cr_2O_3 has largely been oxidized out of the steel with the final composition of 77% Fe, 11% Ni, 6% Cr and other elements in minor concentrations. Thermodynamically this is a two-phase field in the Fe–Ni–Cr–O quaternary system in which the oxygen potential is variable. Taking into account the corresponding boundary systems of Fe–O, Cr–O and Fe–Cr–O, this is between −110 and −137 kcal/mol O_2. At the fuel surface $r = r_0$ (T = 800 K) a zirconium–oxygen phase with values up to 23% oxygen was observed (fig. 6). The oxygen poten-

tial in this phase is approximately −230 kcal/mol O_2 (extrapolated value) according to [14].

The oxygen potential of the fuel at the end of irradiation as calculated from the oxidation state of fission products, steel impurities and the cladding, and the stoichiometry of the fuel determined from this value and by means of thermodynamic data of UO_2 (e.g., [15]) are indicated in table 4 and are plotted in fig. 10 as a function of relative fuel radius. At the end of irradiation, the O/U ratio of the fuel is 2.000 + 0.001 − 0.005 which is constant over the radius.

In every fuel, there exists a shift in stoichiometry during irradiation towards higher values, because the fission products cannot bind all the oxygen released during the fission process. However, calculation of this value for a LWR type fuel is aggravated by uncertainties in fission product yield (broad spectrum of neutron energies), by plutonium fission, which increases nonlinearly during burnup, and also by lack of knowledge of the oxidation state of some fission products. However, for estimates it is possible to use as a basis up to burnups of 5% an average shift in stoichiometry by Δ(O/M) = 0.0013 per % burnup. At a burnup of 4.3% this results in a stoichiometry increase of 0.006. This excess oxygen is completely gettered by the zircaloy cladding, so that the stoichiometry of the fuel assumes the value of either O/U = 2.00 or that of the U–UO_2 phase boundary in the course of irradiation.

It is seen from fig. 7 that a considerable fraction of the oxygen has diffused from the fuel into the zircaloy cladding. On the basis of a concentration profile averaged from the two curves represented and under the assumption that the unknown initial concentration of oxygen in zircaloy is 0.13% the oxygen uptake in a cladding ring 1 mm high is calculated to be 9×10^{18} oxygen atoms. In a UO_2 fuel cylinder 1 mm high (O/U = 2.00), there are 2.9×10^{21} oxygen atoms. It follows from the two values that the fuel would have oxidized from O/U = 2.003 to the final stoichiometry of 2.009 in case of disregarding the gettering effect of zircaloy. Both estimates of the shift in stoichiometry agree well with each other.

Table 4
Oxygen potential and stoichiometry of the fuel at the end of irradiation (EOL)

r/r_0	T (K)	$\Delta\bar{G}_{O_2}$ (kcal/mol)	O/U
0.15	2000	−100 to −90	$2.000\{^{+0.001}_{-0.005}$
0.90	1000	−137 to −110	≤2.00
1	800	≃−230	≤2.00

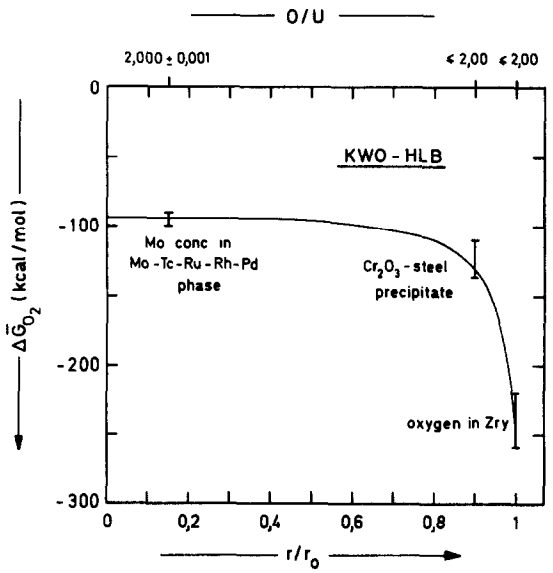

Fig. 10. Chemical oxygen potential of the fuel at the end of live vs. relative fuel radius. It is calculated from the oxidation state of fission products, impurities and the cladding. The corresponding fuel stoichiometry in O/U ratios is indicated at the upper margin of the diagram.

11. Conclusions

In LWR high power fuel rods the O/U ratio of the fuel is mainly determined by the oxygen gettering effect of the zircaloy cladding. The oxygen fraction above the UO_2–Zr(O) equilibrium at the onset of irradiation and that fraction which cannot be bound by the fission products during burnup diffuses into the cladding. The rate of reduction of the fuel is controlled by the rate of oxygen diffusion in the cladding; the stoichiometry is balanced out at an O/U ratio of ≤2.00. The reaction zones between the fuel and the cladding mainly consists of a Cs–Zr–O phase and an α–Zr(O) or ZrO_2 layer; no Cs zirconates were detected. It still needs to be verified experimentally whether the

stoichiometry curve obtained for LWR high power rods agrees with that in LWR standard fuel rods.

Acknowledgements

The author would like to thank KWU Erlangen for making available the specimen, Dr. M. Peehs of KWU for offering some unpublished irradiation data, Mrs. Dr. H. Schneider, KfK, for preparing and conducting the chemical analysis of the zircaloy standards, Mr. H. Keller, KfK, for performing the thermal analysis, and Messrs. H.D. Gottschalg and H. Späte, KfK, for carrying out the studies with the shielded electron-probe microanalyzers.

References

[1] M.G. Adamson, E.A. Aitken, S.K. Evans and J.H. Davies, in: Thermodynamics of Nuclear Materials, Vol. I (IAEA, Vienna, 1974) p. 59.
[2] J. Bazin, J. Jouan and N. Vignesoult, Trans. ANS 20 (1975) 235.
[3] D. Cubicciotti and J.E. Sanecki, J. Nucl. Mater. 78 (1978) 96.
[4] R. Manzel and J. Hartmann, KWU Report RE 23/018/77 (1977).
[5] C.F. Knights and B.A. Phillips, in: 5th Int. Conf. Chemical Thermodynamics, Ronneby, Sweden, 1977; AERE-R 9334 (1979).
[6] D.C. Fee and C.E. Johnson, J. Nucl. Inorg. Chem. 40 (1978) 1375.
[7] H. Kleykamp, J. Nucl. Mater. 66 (1977) 292.
[8] M. Peehs, private communication (1977).
[9] H. Kleykamp, in: Proc. Symp. Advanced LMFBR Fuels, Tucson/Arizona/USA, 1977, p. 166.
[10] H. Kleykamp, in: Proc. Symp. Reaktortagung Hannover, 1978, p. 660.
[11] R. Hoppe and K. Seeger, Z. Anorg. allg. Chem. 375 (1970) 264.
[12] H. Keller, private communication (1978).
[13] J.A.L. Robertson, CRFD–835 (1959).
[14] K.L. Komarek and M. Silver, in: Thermodynamics of Nuclear Materials (IAEA, Vienna, 1962) p. 749.
[15] H. Holleck and H. Kleykamp, Kernforschungszentrum Karlsruhe Report KfK 1181 (1970).
[16] H. Kleykamp, in: Proc. Int. Conf. Fast Breeder Reactor Fuel Performance, Monterey/Calif./USA, 1979, p. 393.